Nerves of Plastic: A Transparent Approach To Distributed Tactile Sensing for Safer Robots

Laura E. Butcher, Chris J. Ford, Nathan F. Lepora, Efi Psomopoulou

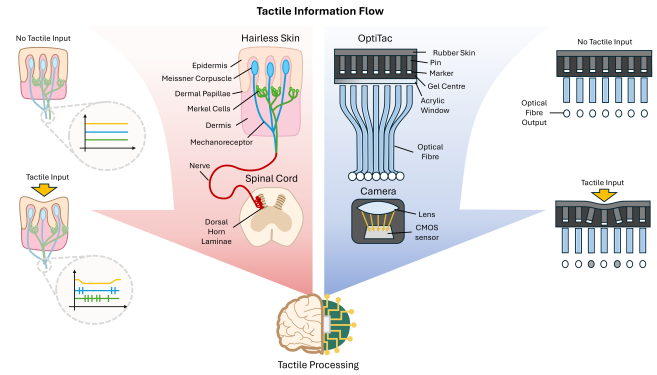

Fig. 1. Concept and bioinspired design of the OptiTac tactile sensor.

I. Introduction

VISION-based tactile sensing includes a strand of research focused on embedding high-resolution touch feedback into robotic fingertips to enhance manipulation capabilities. An example of this is TacTip, a biomimetic vision-based tactile sensor, which has been successfully integrated into robotic fingertips to achieve high levels of robot dexterity [1]. This has been made possible in part by the increased availability of smaller and cheaper cameras [2]. However, human manipulation is not limited to fingertips alone and therefore a distributed tactile sensor is required [3]. Cameras integrated within tactile sensors are limited in their ability to provide distributed tactile sensing, as they can require large focal distances or additional lenses [4].

One way to overcome the scaleability challenges faced by vision-based tactile sensors is to take inspiration from human skin. Nerves transport tactile information away from the skin and terminate in specific regions of the spinal cord (Fig. 1) [5], [6], followed by neurons that transmit these signals to the somatosensory cortex of the brain [7]. This circuitry is thought to play an important role in the processing of tactile signals [8]. Optical fibres (OFs) can act as artificial nerves, transporting tactile information to a remote camera, as they are compact and fast [9]. Combining OF technology with the biomimetic mechanical properties of the TacTip and a single remote camera could be a step towards developing human-like distributed tactile sensing for robots.

To predict key contact parameters, deep learning methods have been applied to tactile data from recently developed OF based tactile sensors [10], [11]. These methods, however, are a ”black-box” in terms of understanding how models are learnt and what influences the model predictions. Alternatively, image moments have been applied to tactile information to extract key contact parameters such as position, orientation, and area [12]–[15], and have been used to complete tasks such as grasp stability [16]. Implementing analytical methods to process tactile information and identify key contact parameters could be a way to minimise the use of non-intuitive methods when factors such as safety are important.

We propose the OptiTac sensor derived from the standard TacTip design (Fig. 1) [17]. Both consist of a soft deformable skin which transduces contact information into visible marker pattern by a levering pin mechanism. A camera is also used in both to digitise the signals. The difference is that OptiTac uses plastic OFs paired with pins to transport tactile information away from the skin to a remote camera. This design decouples the sensing and detection modalities of the TacTip.

II. Method

Pin-OF pairing is a core design principle of OptiTac as it enables the process of transducing contact information. For this design, a distance of 1.5 mm was chosen between neighbouring pairs and a diameter of 1 mm for both the pins and OFs. At rest, the pins on the skin surface align with the respective OFs (Fig. 1 top right). The white markers at the end of the pins result in high intensity of light being transmitted by the OF. When contact occurs, the skin deforms and pins lever, resulting in an unalignment in the pin-OF pairs (Fig. 1 bottom right). The fixed OFs now capture less of the white marker, resulting in a reduction in the intensity of transmitted light due to the skin and pins being black. Encoding visible marker movements into light intensity changes allows for the transmission of tactile information away from the tactile skin.

The image captured by a remote camera is processed to enable the use of simple analytical methods to determine

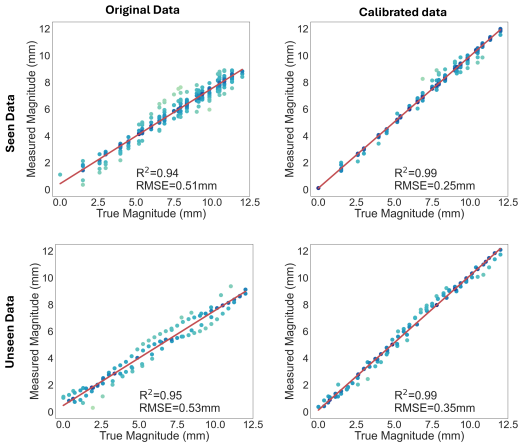

Fig. 2. Contact position calibration results.

Authors are with the School of Engineering Mathematics and Technology, and Bristol Robotics Laboratory, University of Bristol, U.K.

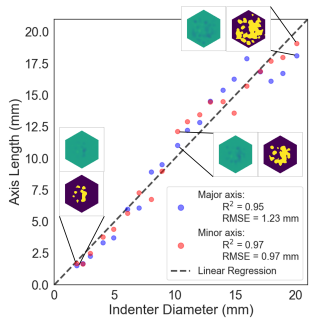

Fig. 3. Contact width results. Some of the resulting surface plots are shown along with a binarised version to highlight the areas of intensity change.

key contact parameters. As the OF positions are fixed, the first camera image can be segmented to find the positions of all OFs. The segmentation results are then applied to the subsequent images to measure the average greyscale pixel value for each OF. These intensity values are then interpolated over the area of the OF positions, producing high resolution surface plots of the output light intensity (Figs. 3, 4a). These surface plots represent the current state of the tactile skin and can be used to measure key contact parameters such as position, width, and shape; we do this using image moments. Raw image moments (m_{ij}) are used to identify the position of the contact's centroid ($\bar{x}, \bar{y}$) with respect to the origin (1).

$$m_{ij} = \sum_x \sum_y x^i y^j I(x,y), \quad \bar{x} = \frac{m_{10}}{m_{00}}, \quad \bar{y} = \frac{m_{01}}{m_{00}}. \quad (1)$$

Central moments are used to calculate the eigenvalues of the intensity distribution which are used to determine the width of the contact (FWHM=$2\sqrt{2\ln h}\sqrt{\lambda}$, where h=2). Hu moments use central moments to perform pattern recognition on distribution shapes [18]. We tested different combinations of the first 7 Hu moments and applied them to the binarised surface plot distributions. A logarithmic transform is then applied, and we classify the values by shape cluster according to a Gaussian Mixture Model (GMM).

III. Results

To evaluate the accuracy of contact position measurement, an indentor was attached to an IRB 120-3/0.6 ABB robot arm, to make repeated indentations of 3 mm depth into the sensor. Initial calibration of the measurement method was needed, which was evaluated by plotting unseen calibrated contact positions against the true contact position. The results show an R^2 of 0.99 and an RMSE of 0.4 mm in both the x- and y-axes (Fig. 2). The RMSE of the contact position measurements is smaller than the distance between neighbouring pin-OF pairs, demonstrating the hyperacuity of the OptiTac sensor.

To evaluate the contact width measurements, a range of 3D printed circular indentors were used to generate contacts of different widths from 1.85 to 20.09 mm in diameter. We performed a secondary calibration so that (a) both the major and minor axes of the contact area have the same value (circular indentation) and (b) when there is no contact, the contact width is 0 mm. As a result, the R^2 values for the major and minor axes were 0.95 and 0.97, respectively, with RMSE values of 1.2 mm and 1.0 mm, respectively (Fig. 3). The RMSE values are smaller than the distance between neighbouring pin-OF pairs, highlighting the effectiveness of interpolation steps and the use of image moments to measure contact width to a sub-pair resolution.

To demonstrate OptiTac's ability to classify different contact shapes, 5 different 3D printed shapes were indented into the sensor skin (Fig. 4a). The 5 shapes (circle, square, triangle, ellipse, and an edge) were indented into the sensor at different orientations and positions. The positions were constrained such that the contact remained within the sensing region. Different combinations of the seven Hu moments were used to generate different GMMs and these models were assessed on their ability to correctly classify shapes. A combination of the first three Hu moments produced the largest average true positive classification of 96 % (Fig. 4b). The chosen Hu moments extracted the relevant features for a GMM to classify the different shapes with minimal errors (Fig. 4c).

IV. Conclusion

Overall, OptiTac builds on the standard TacTip skin design by integrating OFs to transmit tactile information to a remote camera, inspired by the way nerves transmit tactile information away from the skin to the brain. By using a simple design principle of pin-OF pairing, we unlock the potential to scale the sensor and provide distributed tactile sensing. Since the OFs are stationary in the tactile images, a tailored tactile information process was developed rather than relying on "black-box" deep learning methods. This involved using simple image processing techniques to determine key contact parameters. As a result, OptiTac demonstrated hyperacuity, a key property of human skin, and a shape classification model was generated with a visible clustering of shape features. This work marks a step towards the development of scalable bioinspired tactile sensors that can provide distributed intuitive tactile sensing for robots.

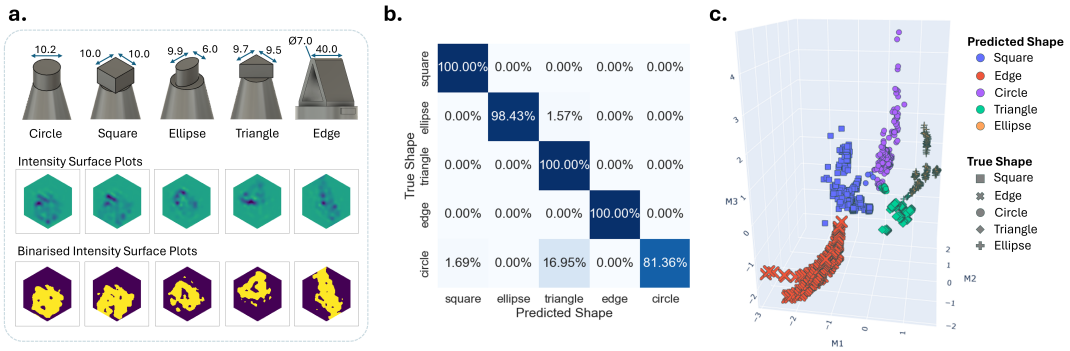

Fig. 4. Contact shape classification results. **a.** The 5 3D printed shapes and their resulting intensity surface plots. **b.** Confusion matrix of chosen Hu moment combination. **c.** Result of GMM classification.

ACKNOWLEDGMENT

This work was supported by the Horizon Europe research and innovation program under grant agreement No. 101120823 (MANiBOT)

REFERENCES

[1] M. Yang, C. Lu, A. Church, Y. Lin, C. Ford, H. Li, E. Psomopoulou, D. A. Barton, and N. F. Lepora, "Anyrotate: Gravity-invariant in-hand object rotation with sim-to-real touch," *arXiv preprint arXiv:2405.07391*, 2024.

[2] N. F. Lepora, "Tactile robotics: Past and future," *The International Journal of Robotics Research*, p. 02783649261421615, 2025.

[3] T. Feix, J. Romero, H.-B. Schmiedmayer, A. M. Dollar, and D. Kragic, "The grasp taxonomy of human grasp types," *IEEE Transactions on human-machine systems*, vol. 46, no. 1, pp. 66–77, 2015.

[4] H. Li, Y. Lin, C. Lu, M. Yang, E. Psomopoulou, and N. F. Lepora, "Classification of vision-based tactile sensors: A review," *IEEE Sensors Journal*, 2025.

[5] V. Abraira and D. Ginty, "The sensory neurons of touch," *Neuron*, vol. 79, no. 4, pp. 618–639, 2013.

[6] J. Turecek, B. P. Lehnert, and D. D. Ginty, "The encoding of touch by somatotopically aligned dorsal column subdivisions," *Nature*, vol. 612, no. 7939, pp. 310–315, 2022.

[7] A. R. Sobinov and S. J. Bensmaia, "The neural mechanisms of manual dexterity," *Nature Reviews Neuroscience*, vol. 22, no. 12, pp. 741–757, 2021.

[8] A. M. Chirila, G. Rankin, S.-Y. Tseng, A. J. Emanuel, C. L. Chavez-Martinez, D. Zhang, C. D. Harvey, and D. D. Ginty, "Mechanoreceptor signal convergence and transformation in the dorsal horn flexibly shape a diversity of outputs to the brain," *Cell*, vol. 185, no. 24, pp. 4541–4559, 2022.

[9] H. Di, Y. Xin, and J. Jian, "Review of optical fiber sensors for deformation measurement," *Optik*, vol. 168, pp. 703–713, 2018.

[10] D. Baimukashev, Z. Kappassov, and H. A. Varol, "Shear, Torsion and Pressure Tactile Sensor via Plastic Optofiber Guided Imaging," *IEEE Robotics and Automation Letters*, vol. 5, no. 2, pp. 2618–2625, Apr. 2020.

[11] Z. Lu, T. Yang, Z. Cao, D. Luo, Q. Zhang, Y. Liang, and Y. Dong, "Optical soft tactile sensor algorithm based on multiscale resnet," *IEEE Sensors Journal*, vol. 23, no. 10, pp. 10 731–10 738, 2023.

[12] A. J. Schmid, N. Gorges, D. Goger, and H. Worn, "Opening a door with a humanoid robot using multi-sensory tactile feedback," in *2008 IEEE international conference on robotics and automation*. IEEE, 2008, pp. 285–291.

[13] N. Gorges, S. E. Navarro, D. Göger, and H. Wörn, "Haptic object recognition using passive joints and haptic key features," in *2010 IEEE International Conference on Robotics and Automation*. IEEE, 2010, pp. 2349–2355.

[14] Q. Li, C. Schürmann, R. Haschke, and H. J. Ritter, "A control framework for tactile servoing." in *Robotics: Science and systems*, 2013.

[15] R. Thomasson, E. Roberge, M. R. Cutkosky, and J.-P. Roberge, "Going in blind: Object motion classification using distributed tactile sensing for safe reaching in clutter," in *2022 IEEE/RSJ International Conference on Intelligent Robots and Systems (IROS)*. IEEE, 2022, pp. 1440–1446.

[16] Y. Bekiroglu, J. Laaksonen, J. A. Jorgensen, V. Kyrki, and D. Kragic, "Assessing grasp stability based on learning and haptic data," *IEEE Transactions on Robotics*, vol. 27, no. 3, pp. 616–629, 2011.

[17] B. Ward-Cherrier, N. Pestell, L. Cramphorn, B. Winstone, M. E. Giannaccini, J. Rossiter, and N. F. Lepora, "The TacTip family: Soft optical tactile sensors with 3d-printed biomimetic morphologies," *Soft Robotics*, vol. 5, no. 2, pp. 216–227, 2018.

[18] M.-K. Hu, "Visual pattern recognition by moment invariants," *IRE Transactions on Information Theory*, vol. 8, no. 2, pp. 179–187, 1962.